

Jet Production and QCD at High Energy Colliders

Dmitry Bandurin^{*†}

Florida State University

E-mail: bandurin@fnal.gov

Selected quantum chromodynamics (QCD) measurements performed at the Fermilab Run II Tevatron $p\bar{p}$ collider ($\sqrt{s} = 1.96$ TeV) by CDF and D0 collaborations, at the LHC pp collider ($\sqrt{s} = 7$ and 8 TeV) by CMS and ATLAS collaborations, and at HERA $e^\pm p$ collider ($\sqrt{s} = 300$ and 314 GeV) by H1 and ZEUS collaborations are presented. The inclusive jet, dijet production and three-jet cross section measurements are used to test perturbative QCD calculations, constrain parton distribution function determinations, and extract values of the strong coupling constant. Events with W/Z +jets production are used to measure many kinematic distributions allowing extensive testing and tuning predictions from next-to-leading-order (NLO) perturbative QCD (pQCD) and Monte-Carlo event generators. The diphoton production cross-sections check the validity of the NLO pQCD predictions, soft-gluon resummation methods implemented in theoretical calculations, and contributions from the parton-to-photon fragmentation diagrams. The photon+ b -jet cross-section measurements reveal an inability of NLO perturbative pQCD calculations to describe spectrum at high transverse momentum. Events with inclusive production of vector boson ($\gamma/W/Z$) and ≥ 2 jets are used to study increasingly important phenomenon of multiple parton interactions, measure an effective interaction cross section, and limit existing models.

36th International Conference on High Energy Physics

4-11 July 2012

Melbourne, Australia

^{*}Speaker.

[†]A footnote may follow.

1. Introduction

QCD, the theory of the strong interaction between quarks and gluons, is heavily tested in experimental studies at hadron colliders. QCD results from the Tevatron obtained with integrated luminosity up to 6 fb^{-1} , LHC up to 5 fb^{-1} , and HERA up to 0.5 fb^{-1} are reviewed in this paper. These results provide a crucial tests for pQCD, information about parton distribution functions (PDFs), measurements of the strong coupling constant, tests for non-perturbative models describing parton fragmentation and multiple parton interactions (MPI). At the same time, the results are used to search for new phenomena and impose limits on the corresponding models.

2. Jet production

Thorough testing of pQCD at short distances is provided through measurements of differential inclusive jet, dijet and three-jet cross sections. The measurements of the inclusive jet cross sections done by the ATLAS [1] and CMS [2] collaborations in a few jet rapidity regions are shown in Fig. 1. In general, they are in agreement within uncertainties with pQCD predictions. Data have about same uncertainties as the theoretical predictions (mostly due to PDF) and can be used to constrain PDFs. Figure 2 shows a comparison of ATLAS data to NLO QCD predictions using CT10 PDF set [3].

The H1 experiment measured inclusive jet, dijet and trijet production cross sections in the Q^2 range from 150 GeV^2 to 15000 GeV^2 , and observed good agreement with NLO QCD predictions using CT10 PDF set [4] (Fig. 3). As shown on the right plot of Fig. 3, jet data are extremely helpful to limit α_s values. Fitting the 42 points of cross section measurements allows one to extract $\alpha_s(M_Z) = 0.1163 \pm 0.0011(\text{exp}) \pm 0.0042(\text{theor})$ with following composition of the relative uncertainties: $\pm 0.9\%$ (exp), $\pm 1.2\%$ (PDFs), $\pm 0.7\%$ (hadronization), $\pm 3.4\%$ (scale), $\pm 3.8\%$ (total). As we see, the theoretical scale uncertainties are dominant. The ZEUS experiment measured inclusive jet cross section in the photoproduction channel ($Q^2 < 1 \text{ GeV}^2$) in five jet rapidity regions (covering $-1 < \eta^{\text{jet}} < 2$) [5]. The measurements were done using k_T , anti- k_T and SIScone algorithms and well described by NLO QCD, except very low and high p_T at high η^{jet} . Using the cross sections measured at $21 < E_T^{\text{jet}} < 71 \text{ GeV}$, α_s values have been extracted. They are presented in Fig.4 (left plot) as a function of E_T^{jet} . A combined fit gives $\alpha_s(M_Z) = 0.1206^{+0.0023}_{-0.0022}(\text{exp})^{+0.0042}_{-0.0035}(\text{theor})$. The $\alpha_s(M_Z)$ values obtained from the measurements with different jet algorithms are consistent with each other and have similar precision. The D0 collaboration introduced a new variable that characterizes angular correlations of jets, and gives an average number of jets around a reference jet [6]. The cross section is measured triple differentially as a function of reference jet p_T , neighboring jet p_T and distance between them ΔR . Systematic uncertainties related with PDF choice are quite small ($< 3\%$). The measurement is used to extract α_s values, which are shown in Fig. 4, right plot. A combined fit results in $\alpha_s(M_Z) = 0.1191^{+0.0048}_{-0.0071}$. A comparison to other experiments is also shown on this plot.

The CDF collaboration studied structure of high p_T jets by selecting only events with at least one jet having $p_T > 400 \text{ GeV}$, $0.1 < |y| < 0.7$ and considering jets with cone sizes $R = 0.4, 0.7$ and 1.0 [7]. Such studies can be used to tune parton fragmentation mechanism and search for heavy resonances decaying hadronically. The jet mass is calculated using 4-vectors of calorimeter towers

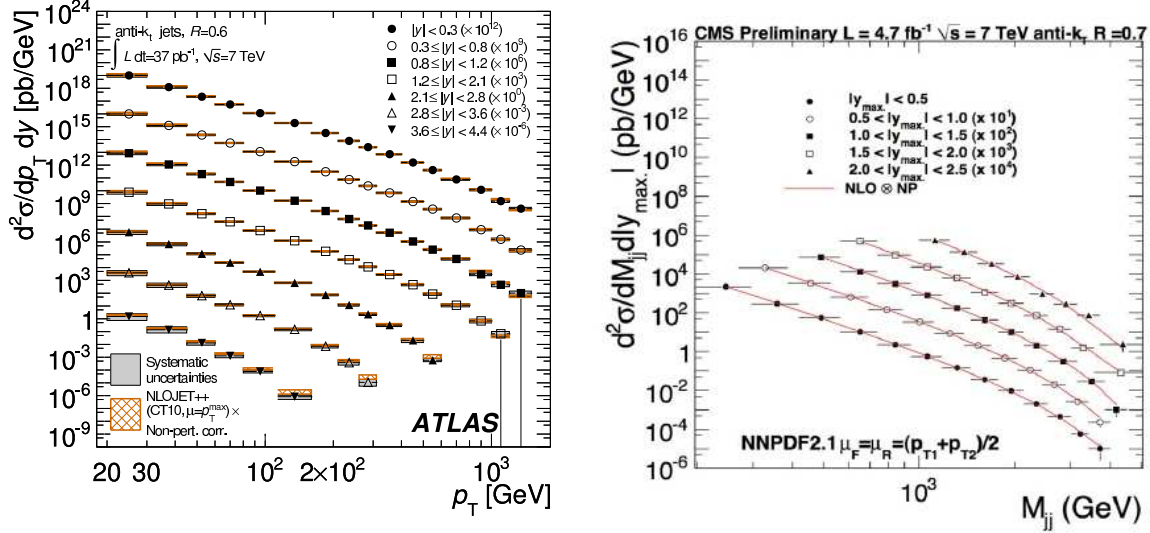


Figure 1: Inclusive jet cross sections measured by ATLAS and CMS collaborations at $\sqrt{s} = 7$ TeV.

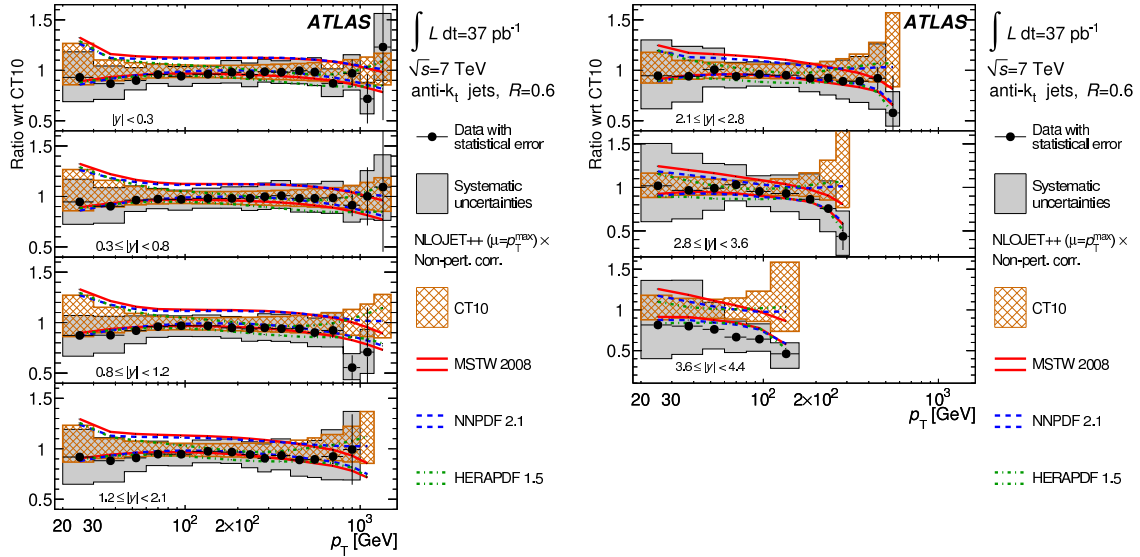


Figure 2: Ratio of inclusive jet cross section measured by ATLAS to NLO QCD predictions in a few jet rapidity bins.

in a jet. Its unfolded distribution obtained with the t -quark rejection cuts is shown on the left plot of Fig. 5. The data are in agreement with PYTHIA predictions and interpolate between the QCD predictions in the leading-log approximation [8] for quark and gluon jets, and confirm that the high mass jets are mostly caused by quark fragmentation. The ATLAS collaboration studied productions of high p_T jets reconstructed with anti- k_T algorithm ($R = 1.0$) [9]. The jets are “trimmed” according to the jet trimming algorithms [10]. The right plot of Fig. 5 shows the jet mass spectrum with a dominant contribution from $t\bar{t}$ events. A bump corresponding to the top-quark mass is clearly seen, and is well described by MC.

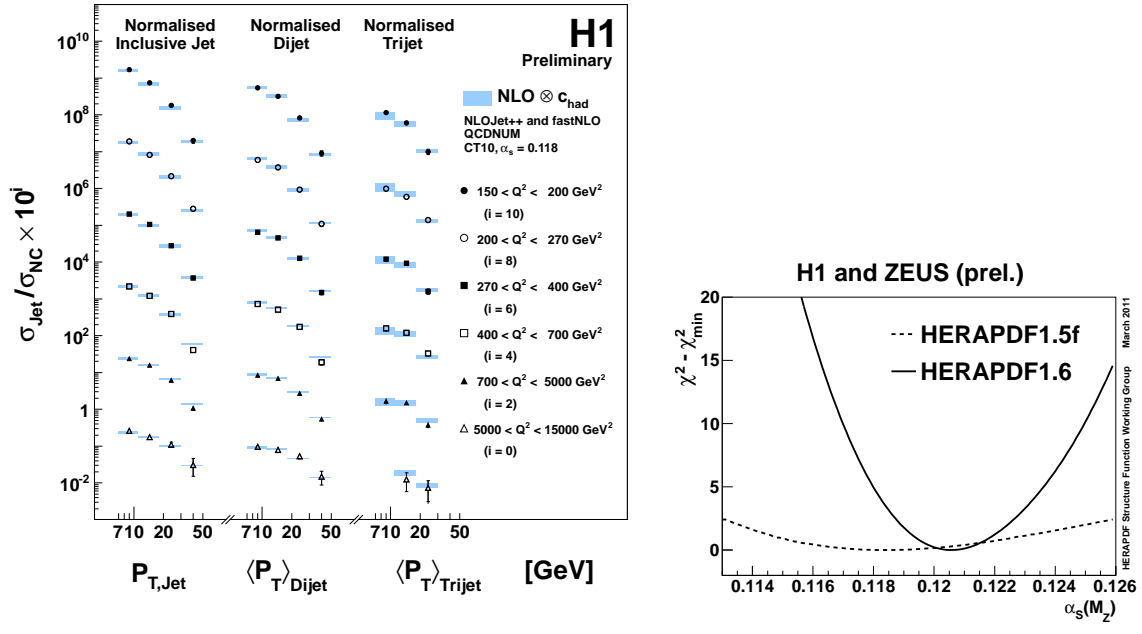


Figure 3: Left: normalized inclusive jet, dijet and trijet cross sections measured by H1 collaboration. Right: χ^2 vs $\alpha_s(M_Z)$ obtained using inclusive DIS data only (dashed line) and inclusive DIS+jet data (solid line).

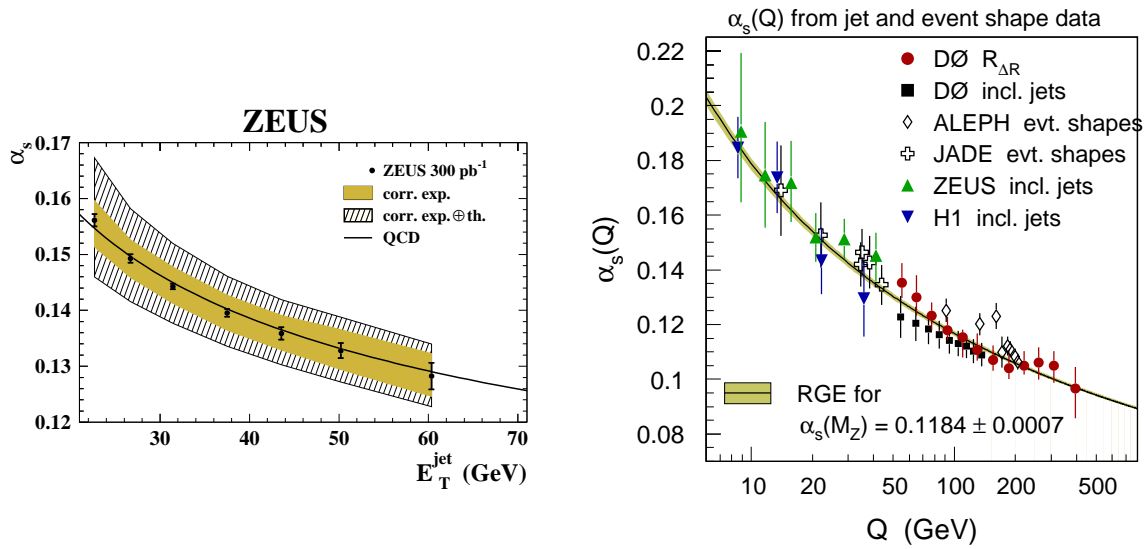


Figure 4: Left: running α_s as a function of jet E_T extracted from ZEUS jet photoproduction data. Right: running α_s extracted using D0 jet, LEP event shapes and HERA jet data.

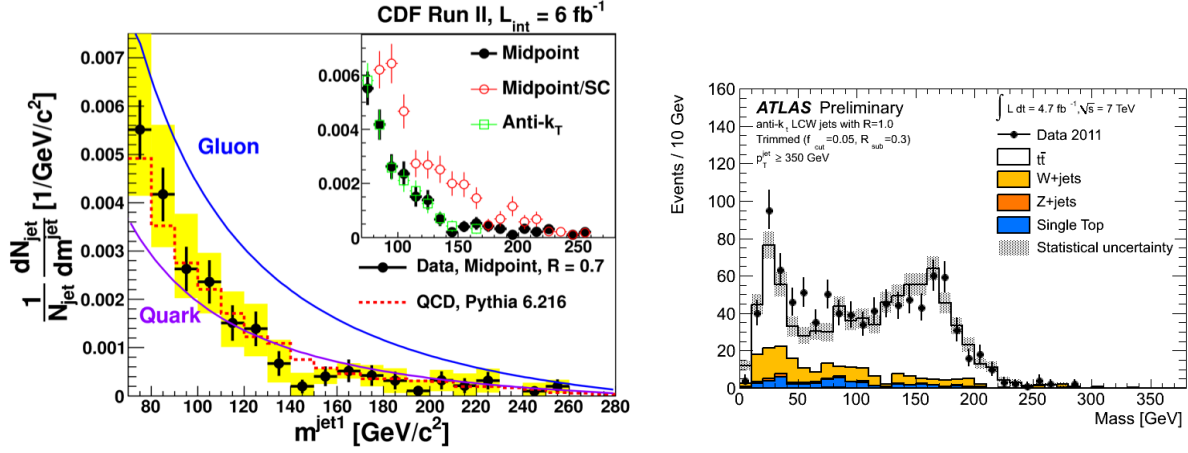


Figure 5: Left: Normalized distribution of jet mass m^{jet} measured at CDF with jet $p_T > 400$ GeV and compared to theory predictions (the inset plot compares m^{jet} distributions with jets found by anti- k_T and midpoint cone algorithms). Left: the m^{jet} spectrum of “trimmed” jets [10] with $p_T > 350$ GeV measured by ATLAS and compared to the theory predictions.

Kinematic distributions characterizing geometric shape of the hadronic final state are sensitive to details of QCD multijet production, but are robust against experimental systematics, e.g. jet energy scale uncertainty. A number of different variables have been studied at the LHC, including aplanarity, transverse thrust, minor component of the transverse thrust, sphericity, and transverse sphericity. The events spectrum for the transverse thrust (τ_\perp) measured by CMS and ATLAS [11, 12] are shown in Fig. 6. High τ_\perp values provide a test of high order pQCD corrections. Potentially, event shapes variables are a source of precise α_s measurements, and have traditionally been used for this in e^+e^- experiments (for example, see [13]).

3. $W/Z + \text{jets}$ production

Tevatron and LHC collaborations have extensively studied $W/Z + \text{jet}$ production since these events are the main background to top-quark, Higgs boson, SUSY and many other new physics production channels. In this section we review some of the latest results.

The left plot of Fig. 7 shows the dijet cross section for $W + \geq 2\text{-jet}$ and $W + \geq 3\text{-jet}$ events measured by D0 collaboration [14]. The measurements are compared to SHERPA MC event generator [15] and NLO pQCD predictions obtained with BLACKHAT+SHERPA [16] and HEJ [17]. The right plot of Fig. 7 shows H_T cross section measured by ATLAS collaboration [18]. The BLACKHAT+SHERPA predictions slightly overestimate rates of $W + \geq 2\text{-jet}$ events at high dijet masses and underestimate rates of $W + \geq 1\text{-jet}$ events at high H_T .

The CDF collaboration measured inclusive differential $Z + b\text{-jet}$ production cross section as a function of $b\text{-jet } p_T$ (Fig. 8) and η [19]. The cross sections are in agreement with NLO QCD predictions done by MCFM [20] and MSTW PDF set [21], except at low jet p_T (20–30 GeV). The CMS collaboration measured $Z + b\text{-jet}$ cross sections differentially versus jet p_T , di- $b\text{-jet } p_T$ (right plot of Fig. 8) and azimuthal angle $\Delta\phi(Z, b)$ [22]. Good agreement with NLO QCD predictions is observed.

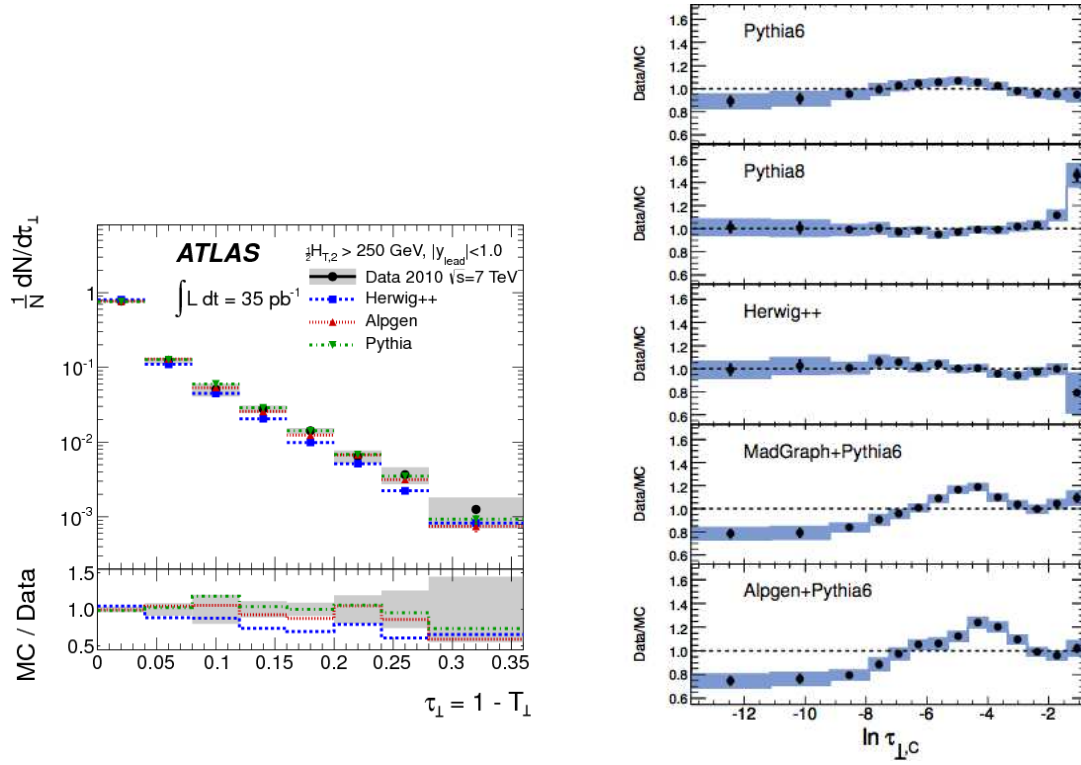


Figure 6: Left: transverse thrust (τ_T) distribution measured by ATLAS and compared to MC generators using jets with rapidity $|\eta| < 1.0$ and mean dijet transverse momentum $0.5H_T > 250$ GeV. Right: ratio of $\ln(\tau_T)$ measured by CMS compared to predictions of different MC generators.

The CDF collaboration measured the cross section of $W + b$ -jet production $\sigma(W + b) \cdot Br(W \rightarrow l\nu) = 2.74 \pm 0.27(\text{stat}) \pm 0.42(\text{syst})$ pb with jet $p_T > 20$ GeV, $|\eta| < 2.0$ and $l = e, \mu$ [23]. The measurement significantly exceeds the NLO prediction 1.2 ± 0.14 pb. The similar $W + b$ -jet cross section was measured by ATLAS [24] to be $10.2 \pm 1.9(\text{stat}) \pm 1.6(\text{syst})$ pb, which is about 1.5 σ higher than NLO QCD predictions $4.8^{+4.8}_{-1.2}(\text{scale})^{+0.3}_{-0.0}(\text{PDF})^{+0.3}_{-0.2}(m_b) \pm 0.3(\text{non-pert. corr.})$.

4. Photon production

Since high p_T photons emerge directly from $p\bar{p}/pp$ collisions and provide a direct probe of the parton hard scattering dynamics, they are of permanent interest in high energy physics. The inclusive photon production cross sections have been measured at the Tevatron [25, 26] and the LHC [27, 28]. They are in agreement within experimental uncertainties with NLO QCD, however one needs to understand discrepancies in shape between LHC and Tevatron data at low p_T^γ . The LHC and Tevatron measurements differ in photon isolation (4–5 GeV at the LHC vs 1–2 GeV at the Tevatron), and parton x_T regions.

In light of the Higgs boson search and searches for other possible resonances decaying to a photon pair, all the collider experiments have performed a thorough study of the diphoton production. The Tevatron and LHC experiments measured the diphoton cross sections as a function of the diphoton mass $M_{\gamma\gamma}$, the transverse momentum of the diphoton system $p_T^{\gamma\gamma}$, the azimuthal angle

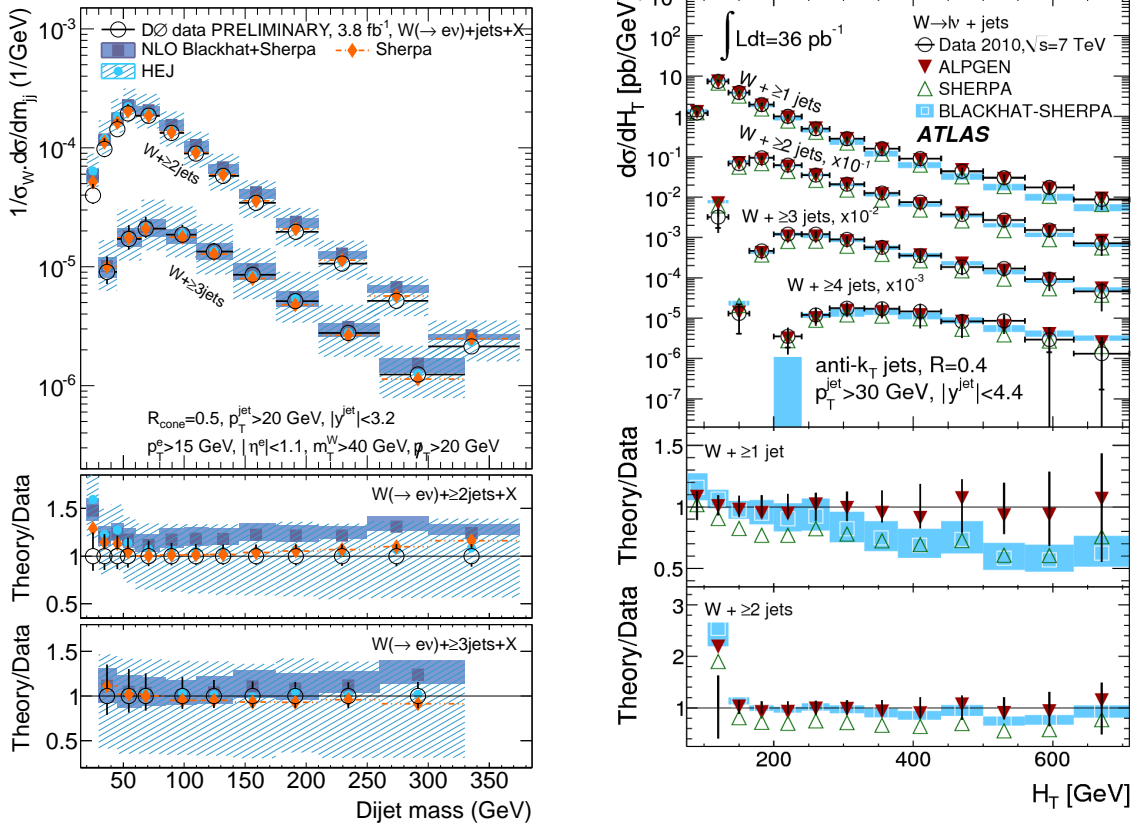


Figure 7: Left: dijet mass spectrum measured by D0 using inclusive $W + \geq 2$ jet and $W + \geq 3$ jet events. Right: jet H_T cross section measured by ATLAS using inclusive $W + \geq 1$ jet and $W + \geq 2$ jet events.

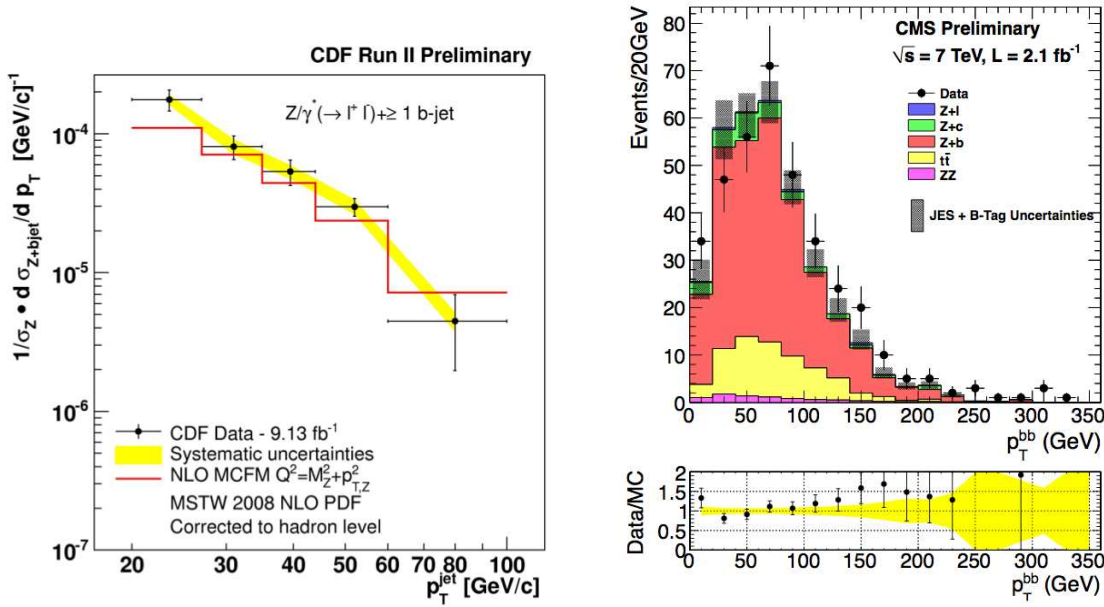


Figure 8: Left: differential b -jet p_T cross section measured by CDF in $Z + \geq 1b$ -jet events. Right: net di- b -jet p_T measured by CMS using $Z + \geq 2b$ -jet events.

POS (ICHEP2012) 003

between the photons $\Delta\phi_{\gamma\gamma}$, and the polar scattering angle of the photons. The measurements are typically compared to NLO QCD using RESBOS [33] and DIPHOX [34], NNLO QCD using 2γ NNLO [35], and SHERPA [15] predictions. The results show that the largest discrepancies between data and NLO predictions for each of the kinematic variables originate from the lowest $M_{\gamma\gamma}$ region ($M_{\gamma\gamma} < 50$ GeV), where the contribution from $gg \rightarrow \gamma\gamma$ is expected to be largest [29]. As shown in [30], the discrepancies between data and the theory predictions are reduced in the intermediate $M_{\gamma\gamma}$ region, and a quite satisfactory description of all kinematic variables is achieved for the $M_{\gamma\gamma} > 80$ GeV region which is the relevant region for Higgs boson and new phenomena searches. None of the models describe the data well in all kinematic regions, in particular at low diphoton mass ($M_{\gamma\gamma} < 60$ GeV), low $\Delta\phi_{\gamma\gamma}$ (< 1.7 rad) and moderate $p_T^{\gamma\gamma}$ (20 – 50 GeV) [29, 30, 31]. Figure 9 shows $M_{\gamma\gamma}$ cross section measured by CMS and $p_T^{\gamma\gamma}$ measured by D0 collaborations.

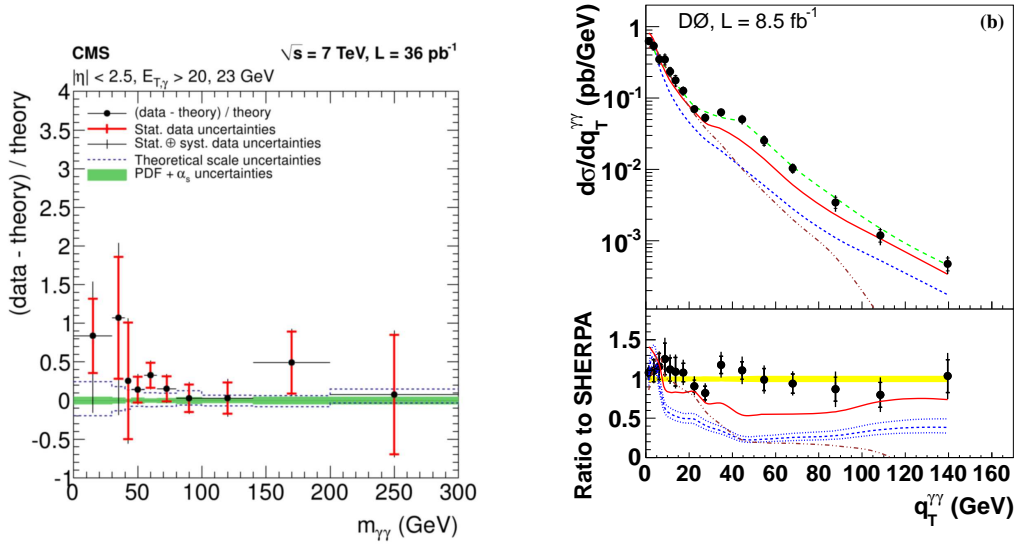


Figure 9: The differential diphoton production cross sections as functions of $M_{\gamma\gamma}$ measured by CMS (left) and $p_T^{\gamma\gamma}$ measured by D0 (right). The CMS data are compared to the theoretical predictions done with DIPHOX [34]; the D0 data and compared to SHERPA (green line) 2γ NNLO (red line) [35], DIPHOX and RESBOS [33]. In the bottom plots, the scale uncertainties are shown by dash-dotted lines and the PDF uncertainties by shaded regions.

The photon+heavy flavor jet final state is sensitive to b/c -quark PDFs (at low p_T^{γ}) and contributions from the annihilation diagrams with $g \rightarrow Q\bar{Q}$ splitting (at high p_T^{γ}). Figure 10 shows $\gamma + b$ and $\gamma + c$ cross sections measured by CDF and D0 [36, 37], compared to NLO QCD predictions [38]. The measured $\gamma + b$ cross sections are higher than the predictions at moderate and high p_T^{γ} and require higher order corrections in the theory.

5. Multiple parton interactions

The Tevatron experiments comprehensively studied the phenomenon of multiple parton interactions (MPI) with a multijet final state in a few measurements [39, 40, 41]. Both CDF and D0 found that rates of events with double parton (DP) hard scatter interactions in $\gamma + 3$ jet final

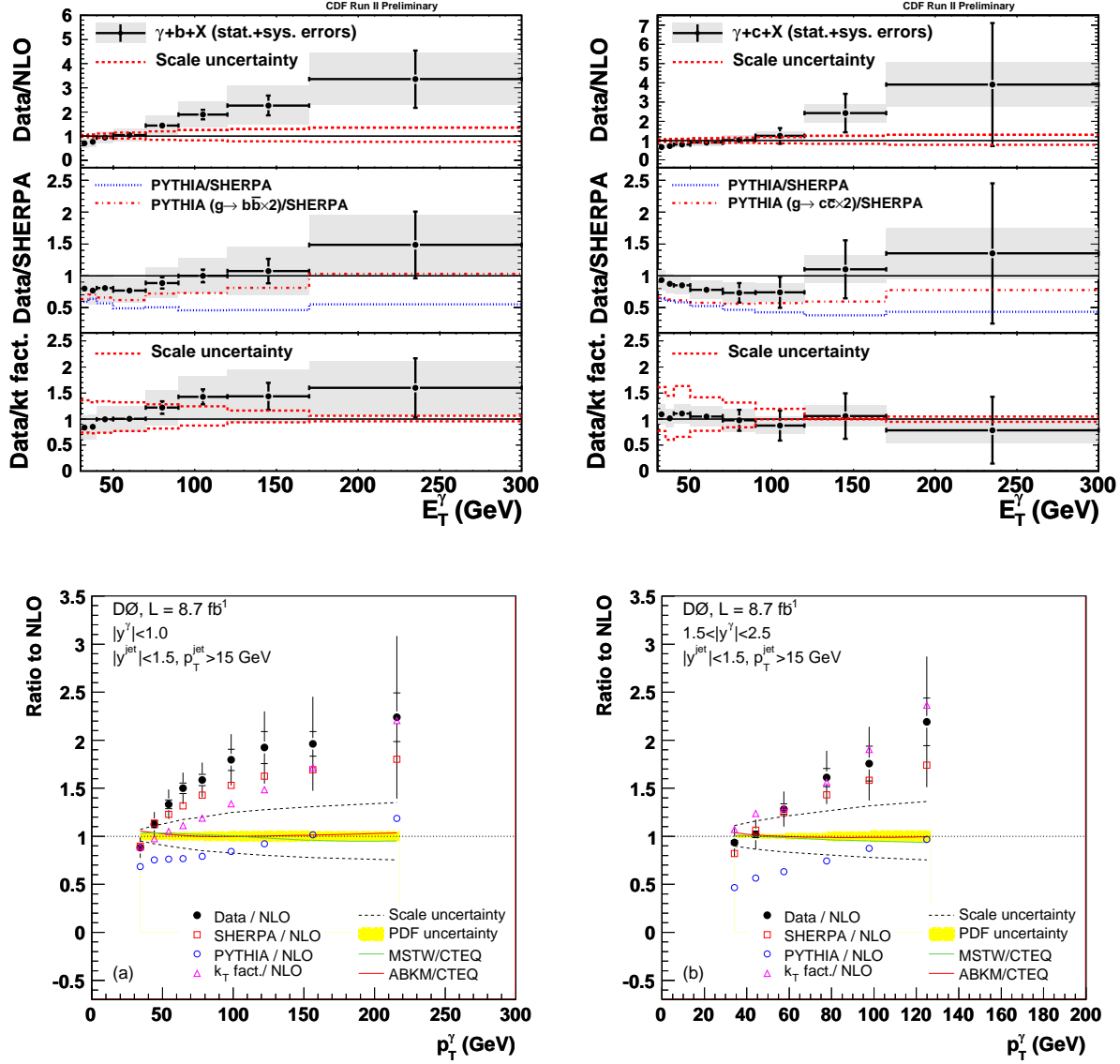


Figure 10: Top: the $\gamma+b$ (left) and $\gamma+c$ differential cross section measured by CDF. Bottom: the $\gamma+b$ differential cross section with photon in central (left) and forward (right) rapidity regions measured by D0.

state can be quite large (up to $\sim 50\%$ at jet $p_T \simeq 15 - 20$ GeV). The D0 collaboration measured the effective cross section $\sigma_{\text{eff}} = 16.4 \pm 0.3(\text{stat}) \pm 2.3(\text{syst})$ that characterizes rates of DP events, $\sigma_{\text{DP}}^{\gamma j, jj} = \sigma^{\gamma j} \sigma^{jj} / \sigma_{\text{eff}}$. This result is in agreement with the previous CDF measurement [39]. Using the inclusive $W + 2$ -jet final state with jet $p_T > 20$ GeV, the ATLAS collaboration measured the fractions of DP events [42]. They are shown in Fig. 11 as a function of jet p_T . The relative vector p_T imbalance of the two jets has been used to discriminate between DP and single parton (SP) interactions. To calculate such an imbalance in the former sample, dijet events from real data have been used. To model SP events, MC events are simulated using SHERPA and ALPGEN+HERWIG+JIMMY generators. Having the DP fractions determined, ATLAS found $\sigma_{\text{eff}} = 15 \pm 3(\text{stat})_{-3}^{+5}(\text{syst})$. The

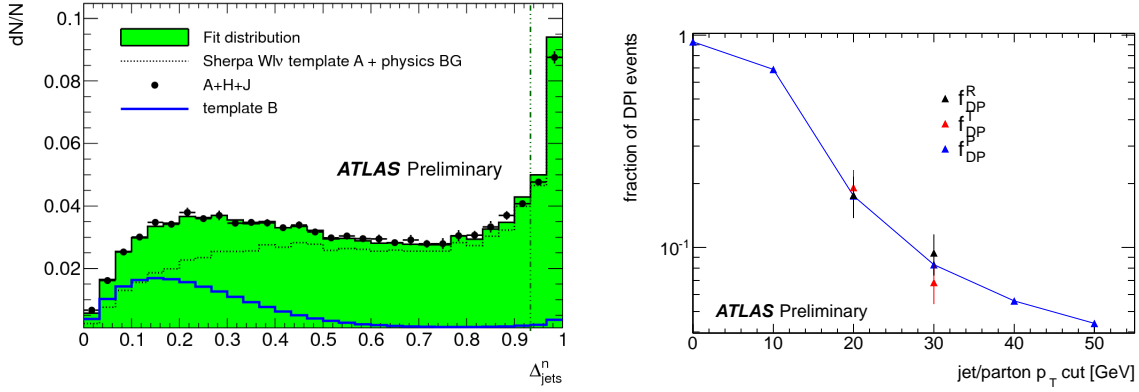


Figure 11: Left: distribution over a discriminant variable in $W + 2$ -jet events in ATLAS data, compared with those in the events with double parton and single parton scatterings. Right: fractions of double parton events as a function of jet p_T .

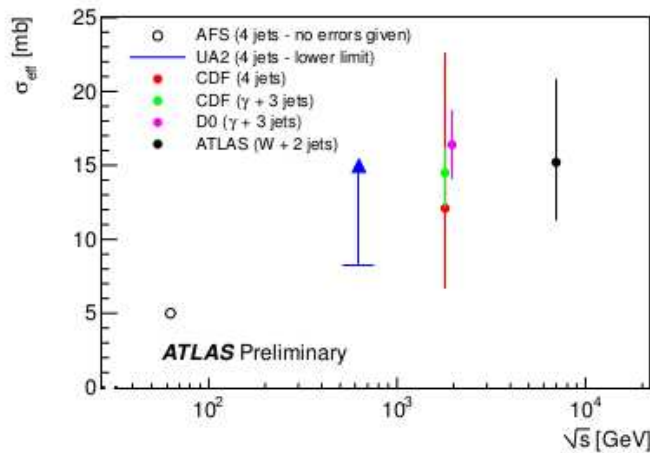


Figure 12: The world results on the measurements of effective cross section σ_{eff} .

effective cross sections measured in the world so far are shown in Fig. 12. More measurements are needed to check dependence of σ_{eff} on energy and initial parton flavors.

6. Summary

The Tevatron, LHC and HERA experiments provide precision QCD measurements of many fundamental observables. For the most part, the results are mutually consistent or complementary to each other. Jet measurements show good agreement with pQCD, and sensitivity to PDF sets, they provide the strongest constraint on the high- x gluon PDF, are used to extract α_s , study jet substructure, and provide limits on many new phenomena models. The W/Z +jets results provide extensive tests of pQCD and tune existing MC models. The photon results test fixed order NLO pQCD predictions accounting for resummation and fragmentation effects and show that the

theory should be better understood. Study of MPI events impose strong constraints and improve phenomenological MPI models at low and high p_T regimes.

References

- [1] G. Aad *et al.* (ATLAS), Phys.Rev. **D86** (2012) 014022.
- [2] S. Chatrchyan *et al.* (CMS), CMS-PAS-QCD-11-004, Phys.Rev.Lett. **107** (2011) 132001.
- [3] P. M. Nadolsky *et al.*, Phys. Rev. D **78** 013004 (2008).
- [4] F. D. Aaron *et al.* (H1), H1prelim-12-031.
- [5] H. Abramowicz *et al.* (ZEUS), DESY-12-045.
- [6] V. M. Abazov *et al.* (D0), Phys.Lett. B **718**, 56 (2012).
- [7] T. Aaltonen *et al.* (CDF), CDF Note CDF-10199 (2011).
- [8] L. G. Almeida *et al.*, Phys.Rev. D **79** 074017 (2009).
- [9] G. Aad *et al.* (ATLAS), ATLAS-CONF-2012-065, JHEP **05**, 128 (2012).
- [10] D. Krohn, J. Thaler, and L.-T. Wang, JHEP **02**, 084 (2010).
- [11] S. Chatrchyan *et al.* (CMS), JHEP **06**, 160 (2012).
- [12] S. Chatrchyan *et al.* (CMS), Eur.Phys. J. **C72** 2211 (2012).
- [13] G. Dissertori *et al.*, JHEP **08**, 036 (2009).
- [14] V. M. Abazov *et al.* (D0), Phys. Lett. B **705**, 200 (2011).
- [15] T. Gleisberg *et al.*, JHEP **02**, 007 (2009).
- [16] C. F. Berger *et al.*, arXiv:0905.2735 [hep-ph].
- [17] J. R. Andersen and J. M. Smillie, JHEP **06**, 010 (2011).
- [18] V. M. Abazov *et al.* (ATLAS), Phys. Rev. D **85**, 092002 (2012).
- [19] T. Aaltonen *et al.* (CDF), Phys.Rev. D **79**, 052008 (2009).
- [20] R. K. Ellis *et al.*, JHEP **01**, 012 (2009).
- [21] A. D. Martin, W.J. Stirling, R.S. Thorne, G. Watt, Eur. Phys. J. C **63** 189 (2009).
- [22] S. Chatrchyan *et al.* (CMS), JHEP **06**, 126 (2012).
- [23] T. Aaltonen *et al.* (CDF), Phys.Rev.Lett. **10**, 131801 (2010).
- [24] G. Aad *et al.* (ATLAS), Phys.Lett. **B707** 418 (2012).
- [25] V.M. Abazov *et al.* (D0), Phys.Lett. B **639**, 151 (2006); *ibid.* **658**, 285 (2008).
- [26] T. Aaltonen *et al.* (CDF), Phys. Rev. D **80**, 111106 (2009).
- [27] S. Chatrchyan *et al.* (CMS), Phys. Rev. D **84** (2011) 052011.
- [28] G. Aad *et al.* (ATLAS), Phys.Lett. B **706** 150 (2011).
- [29] V. M. Abazov *et al.* (D0), Submitted to Phys. Lett. B.
- [30] V. M. Abazov *et al.* (D0), Phys. Lett. B **690**, 108 (2010).

- [31] T. Aaltonen *et al.* (CDF), CDF Note CDF-10160 (2011).
- [32] T. Sjöstrand, S. Mrenna, P. Z. Skands, JHEP **05**, 026 (2006).
- [33] C. Balazs, E. L. Berger, P. Nadolsky, and C.-P. Yuan, Phys. Rev D **76**, 013009 (2007).
- [34] T. Binoth, J. Ph. Guillet, E. Pilon, and M. Werlen, Eur. Phys. J. C **16**, 311 (2000).
- [35] S. Catani, L. Cieri, D. Florian, G. Ferrera, and M. Grazzini, Phys. Rev. Lett. **108**, 072001 (2012).
- [36] T. Aaltonen *et al.* (CDF), CDF Note CDF-10818 (2012).
- [37] V.M. Abazov *et al.* (D0), Phys.Lett. B **714**, 32 (2012).
- [38] T. Stavreva and J.F. Owens, Phys. Rev. D **79**, 054017 (2009).
- [39] F. Abe *et al.* (CDF), Phys.Rev. D **56**, 3811 (1997).
- [40] V. M. Abazov *et al.* (D0), Phys.Rev. D **81**, 052012 (2010).
- [41] V. M. Abazov *et al.* (D0), Phys.Rev. D **83**, 052008 (2011).
- [42] G. Aad *et al.* (ATLAS), ATLAS-CONF-2011-160.